The Astrophysical Journal Letters, 735:L6 (5pp), 2011 July 1 doi:10.1088/2041-8205/735/1/L6

DISTRIBUTION FUNCTIONS OF SIZES AND FLUXES DETERMINED FROM SUPRA-ARCADE DOWNFLOWS

D. E. McKenzie[1] and S. L. Savage[2]
[1] Department of Physics, P.O. Box 173840, Montana State University, Bozeman, MT 59717-3840, USA
[2] NASA/Goddard Space Flight Center, Oak Ridge Associated Universities, 8800 Greenbelt RD, Code 671, Greenbelt, MD 20771, USA
Received 2011 February 18; accepted 2011 May 19; published 2011 June 3

ABSTRACT

The frequency distributions of sizes and fluxes of supra-arcade downflows (SADs) provide information about the process of their creation. For example, a fractal creation process may be expected to yield a power-law distribution of sizes and/or fluxes. We examine 120 cross-sectional areas and magnetic flux estimates found by Savage & McKenzie for SADs, and find that (1) the areas are consistent with a log-normal distribution and (2) the fluxes are consistent with both a log-normal and an exponential distribution. Neither set of measurements is compatible with a power-law distribution nor a normal distribution. As a demonstration of the applicability of these findings to improved understanding of reconnection, we consider a simple SAD growth scenario with minimal assumptions, capable of producing a log-normal distribution.

Key words: magnetic reconnection – Sun: corona – Sun: flares – Sun: X-rays, gamma rays

1. INTRODUCTION

Supra-arcade downflows (SADs) are downward-moving features observed in the hot, low-density region above posteruption flare arcades. Initially detected with the *Yohkoh* Soft X-ray Telescope (SXT) as X-ray-dark, blob-shaped features, downflows have since been identified in many flares, with a variety of instruments (McKenzie 2000; Innes et al. 2003; Khan et al. 2007; Savage & McKenzie 2011). Descriptions of their characteristics, with example movies, are provided by McKenzie (2000); discussion of semi-automated routines for detecting and tracking SADs can be found in McKenzie & Savage (2009). The darkness of these features in X-ray and extreme-ultraviolet (EUV) images and spectra, and their lack of absorption signatures in EUV, indicate that the SADs are best explained as pockets of very low plasma density or plasma voids (see especially Innes et al. 2003). Although SADs of the plasma void type were the first to be identified (McKenzie & Hudson 1999), numerous instances of shrinking loops have also been reported (McKenzie 2000; McKenzie & Hudson 2001). Savage et al. (2010) introduced the moniker SADLs (supra-arcade downflowing loops) for downflows of this latter type. Interpreting both types as shrinking post-reconnection flux tubes, McKenzie & Savage (2009) utilized the measured cross-sectional area of plasma voids and an estimate of the magnetic flux density to assign an estimated magnetic flux to each shrinking tube. The flux estimated in this way, $\sim 10^{18}$ Mx, is notably similar to the flux reported by Longcope et al. (2005), found by a different means.

In Savage & McKenzie (2011), the authors presented measurements of SADs and SADLs sampled from a large number of solar flares observed with *Yohkoh*/SXT, *Transition Region and Coronal Explorer* (*TRACE*), *Hinode*/X-Ray Telescope (XRT), and *Solar and Heliospheric Observatory*/Large Angle and Spectromeric Coronagraph Experiment (*SOHO*/LASCO). In the present Letter, we attempt to infer from the frequency distributions of SAD sizes and magnetic fluxes information about the process(es) responsible for creation of the SADs. Such a study is the natural extension of the ensemble characteristics presented by Savage & McKenzie (2011), and the findings have implications for an improved understanding of the formation of SADs, and perhaps for numerical modeling of patchy magnetic reconnection. For example, the fractal current sheet proposal of Shibata & Tanuma (2001) would tend to yield copious numbers of smaller and smaller magnetic islands forming in the current sheet in a scale-invariant cascade. The frequency distribution of sizes, and perhaps fluxes, of magnetic islands in such a fractal current sheet is expected to tend toward a power-law distribution. Nishizuka et al. (2009) analyzed small-scale brightenings in the 2000 July 14 "Bastille Day" flare, and found that a power-law distribution produced a good fit to the "peak intensity, duration, and time interval" of the time profiles of the brightenings. Nishizuka et al. (2009) interpreted the power-law distribution as possible evidence supporting the fractal current sheet concept. Similarly, Aschwanden et al. (1998) fitted curves to a very large sample (tens of thousands) of hard X-ray pulses, radio Type III bursts, and decimetric pulsations and spikes, all interpreted as signatures of elementary energy release events. Aschwanden et al. (1998) deduced for each burst the peak energy dissipation rate and then explored the frequency distribution of those energy fluxes. Those authors found that a power-law distribution provided a satisfactory representation of the whole sample; on the other hand, analysis of bursts in individual flares suggested that while power-law distributions provided good fits for the hard X-ray pulses and Type III bursts in many flares, the decimetric pulsations and decimetric millisecond spikes were better fit by exponential distribution functions. Aschwanden et al. (1998) suggested that the variations in frequency distribution may be related to differences in the relevant emission sources.

In a model of island formation in current sheets, Fermo et al. (2010) determined an analytic expression for the expected frequency distribution of fluxes and radii of islands, including consideration of possible merging of the islands. For the case of very little merging, Fermo et al. (2010) found that the frequency distribution resembles a decaying exponential. In a separate study, Drake et al. (2010) simulated islands in stacked current sheets in the heliosheath, a simulation which included merging of the islands into "bubbles." Opher et al. (2011) present a description of the evolution of these "bubbles" and find (non-rigorously) that the frequency distribution of magnetic field intensities within the bubbles roughly resembles a log-normal distribution.

In the following sections, we compare the measured areas and fluxes from Savage & McKenzie (2011) to some common statistical distribution functions in an effort to draw inferences

Table 1
List of Flares Analyzed in This Work

Date	Time of SADs (UT)	GOES Class.	Number of SADs
1998 Apr 23	06:00–07:10	X1.2	10
1998 Apr 27	09:42–11:50	X1.0	7
1998 May 9	05:07–05:39	M7.7	3
1998 Sep 30	13:40–13:52	M2.9	5
1998 Nov 23	11:53–12:27	M3.2	5
1999 Jan 20	20:36–22:58	M5.2	25
1999 May 3	06:06–06:30	M4.4	14
1999 Jul 25	13:35–13:56	M2.4	6
1999 Nov 28	20:39–22:08	M1.6	6
2000 Feb 22	20:28–21:11	M1.1	6
2000 Jul 12	21:16–21:47	M1.9	10
2000 Nov 8	23:24–23:27	M7.5	2
2001 Apr 3	03:43–06:51	X1.2	5
2001 Jun 26	15:33–18:48		9
2001 Oct 30	19:05–20:39	C5.0	3
2001 Nov 1	14:50–16:10	M1.8	4

about their formation. The final distribution of SAD sizes is of course affected by the processes of creation and growth, and may also be affected by subsequent fragmentation into smaller voids, and merging of voids. Although fragmentation and merging may be possible for SADs, these events have not been unambiguously observed in coronal images to date. Future observations may provide evidence for fragmentation and/or merging, allowing empirical estimation of their relative importance; we will not consider these effects herein. Pursuant to the interpretation of the SADs/SADLs as reconnection products, it is thus conjectured that the sizes and magnetic fluxes yield information about the rate of reconnection in the individual flux transfer events. We find that a log-normal distribution appears to best fit the SAD sizes and is also consistent with the SAD fluxes. We provide a simple interpretation, with minimal assumptions, to indicate one way a log-normal distribution might result from the growth of the plasma voids.

2. MEASUREMENTS AND DISTRIBUTIONS

The measurements of Savage & McKenzie (2011) include SADs and SADLs from more than one instrument and more than one flare. In that work, the SADLs in any one flare were all assigned the same diameter, a choice that was necessitated by the data. In the present work, we consider only the SADs (i.e., downflows of the plasma void type), since the areas were determined from signal thresholds in the images. Furthermore, we examine only the 120 SADs found with *Yohkoh*/SXT, in order to avoid instrument-dependent variations in the distributions that arise when the data from multiple telescopes are combined. The angular resolution for most of the SXT observations is 4.91 arcsec pixel^{-1} (SXT's "half-resolution"), corresponding to an area unit of approximately 12.5 Mm^2 pixel^{-1}. SADs in the 2001 June 26 flare were analyzed with "full resolution," 2.455 arcsec pixel^{-1}. For each of the SADs discussed herein, the area is found by averaging multiple measurements made during the SAD's lifetime.

The *TRACE* observations listed by Savage & McKenzie (2011) have the benefit of higher spatial resolution, but comprise a much smaller sample—all 23 SADs are from a single flare. On the other hand, the SXT data have the benefit of a larger sample, but are drawn from 16 flares (listed in Table 1). In order to produce a sample large enough for a meaningful examination of the frequency distribution, we combine the 120 SXT SADs into a single set, even though this introduces two related assumptions. First is the assumption that the spectrum of SAD sizes and/or fluxes is the same for all the flares. To a degree this seems reasonable, as it supposes that the processes which add/remove flux to a given flux tube are the same in each flare. We presume that each flux tube is created by a burst of three-dimensional reconnection, and that each burst is independent of other bursts. Thus, the essence of the primary assumption is that reconnection proceeds in a similar way in each flare, or at least that the products of reconnection are similar in each flare.

The second assumption is that SADs are detected equally well in all the flares. All SADs were initially found with an automated detection program and had signals darker than their surroundings by at least 1.1 standard deviations. Each was subsequently verified by visual inspection. Owing to the contrast enhancement performed as part of the data preparation, there is no statistical correlation between detection threshold and measured SAD area. As a test of the effect on detectability due to the brightness of background signal in the images, we asked if smaller SADs are detected less frequently in more intense flares. To examine this question we grouped the SADs into four bins, according to the GOES classification of the flares. The bins are as follows: Group 1 includes SADs from flares with GOES C5.0 through M1.9, Group 2 includes GOES M2.4–M4.4, Group 3 includes a single flare with GOES M5.2, and Group 4 includes GOES M7.5–X1.2. The 2001 June 26 SADs are not included in this binning, since that event occurred beyond the limb and did not have a recorded GOES classification. Examining the frequency distributions in these subsets, we see no clear evidence for a systematic observational bias—the frequency distributions for the four groups are roughly similar, with reasonable variation due to the small samples. Importantly, small SADs are found both in the largest and smallest flares. Therefore, we proceed with analysis of the combined set of SAD measurements, although the results should be interpreted with consideration of the underlying assumptions.

For the set of SAD area measurements, and for the set of SAD flux estimates, we show the frequency distributions in Figures 1(a) and 2(a). As also mentioned in Savage & McKenzie (2011), the distributions show a greater number of smaller sizes/fluxes than larger ones. The downturn of frequency distribution for the smallest size/flux bins is a characteristic of a log-normal distribution. Plots of the frequency distributions for ln(area) and ln(flux) indicate normal-like distributions as well (and thus suggest log-normal distributions of size and flux), but are omitted here in the interest of space. In Figures 1(a) and 2(a), a log-normal distribution is overplotted for comparison; Figure 2(a) also displays an exponential curve for comparison. The shape of the log-normal curve is defined by the mean and standard deviation of the data, and the exponential curve is defined fully by the mean of the data. Therefore, the curves in Figures 1(a) and 2(a) should be considered fits only to the extent that they produce the same mean, standard deviation, and total number of SADs as the data. For a more quantitative diagnostic of the distributions we construct the cumulative distribution of the data in Figures 1(b) and 2(b), which are then compared to the analytic cumulative distribution functions (CDFs) of four common statistical distributions: normal, log-normal, exponential, and power law. In each figure, the cumulative distribution of the data sample is shown as diamond-shaped symbols.

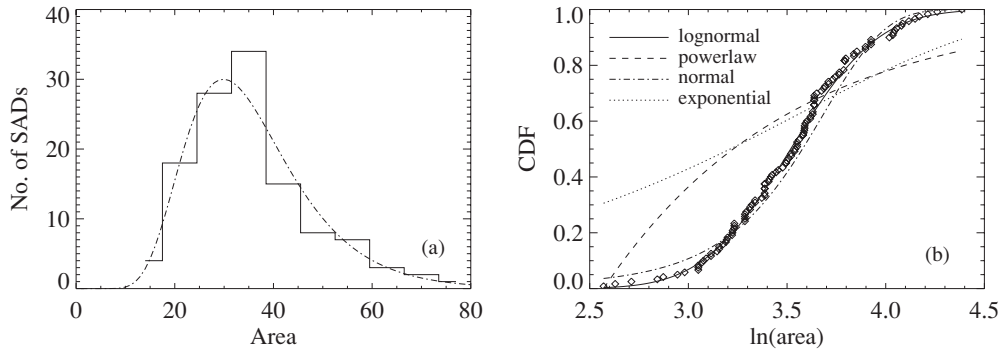

Figure 1. Distribution of SAD areas. (a) Measured frequency distribution of SAD sizes, in units of Mm^2. A log-normal distribution curve is overlaid for comparison. (b) Cumulative distribution of SAD sizes as diamond-shaped symbols, overplotted with theoretical CDFs.

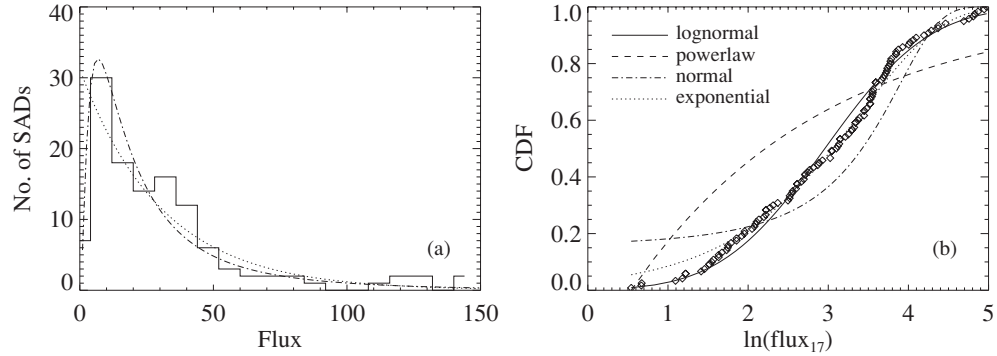

Figure 2. Distribution of estimated SAD fluxes. (a) Frequency distribution of fluxes. Overplotted curves show a log-normal distribution (dash-dotted) and an exponential distribution (dotted) for comparison. (b) Cumulative distribution of fluxes as diamond-shaped symbols, overplotted with theoretical CDFs. In both panels, the fluxes have been normalized by 10^{17} Mx.

Table 2
Goodness-of-fit Parameters Calculated via the Kuiper Variant of the Kolmogorov–Smirnov Test, for each of Four Distribution Functions

Sample	Log-normal Distribution	Power Law	Normal	Exponential
SAD area	$D = 0.097$	$D = 0.499$	$D = 0.187$	$D = 0.527$
	sig = 0.71	sig = 3.9×10^{-25}	sig = 5.7×10^{-3}	sig = 3.2×10^{-28}
SAD flux	$D = 0.128$	$D = 0.416$	$D = 0.333$	$D = 0.126$
	sig = 0.25	sig = 3.8×10^{-17}	sig = 1.4×10^{-10}	sig = 0.27

Note. Small significance values (e.g., $\lesssim$0.10) indicate that the CDF is not compatible with the data.

To test the goodness of fit for each of the proposed CDFs, we employed the Kuiper variant of the Kolmogorov–Smirnov test. According to Press et al. (1992), the traditional Kolmogorov–Smirnov tends to be most sensitive to deviations in the middle of a CDF's range, and least sensitive at the extrema. We elected to use the Kuiper variant in order to preserve sensitivity to deviations throughout the full range of the CDF. The Kuiper significances of the CDF comparisons are listed in Table 2. As in the traditional Kolmogorov–Smirnov test, small values of the significance indicate that the CDFs are incompatible. From these significances, we infer the following: (1) The SAD areas are consistent only with a log-normal distribution. (2) The SAD fluxes are inconsistent with a normal or power-law distribution, but consistent with both log-normal and exponential distributions.

As an additional test, we repeated the area analysis omitting the SADs measured in the 2001 June 26 flare. This flare contributes the majority of SAD areas smaller than 20 Mm^2, and therefore one may reasonably ask if the overall distribution is affected by their inclusion/exclusion. We find that the result is unchanged: the areas of the other 111 SADs are consistent with a log-normal distribution (with Kuiper significance 0.4), and the other distributions are ruled out completely (significances between 5×10^{-4} and 6×10^{-31}).

Finally, we examined the 25 SADs from the 1999 January 20 flare (i.e., Group 3). Though the sample is much smaller, we find that the areas are consistent with a log-normal distribution (significance 0.3), and less likely to be normally distributed (significance 8×10^{-2}). Power-law and exponential distributions are discounted with significances 2×10^{-3} and 6×10^{-8}, respectively.

Although the *TRACE* data of Savage & McKenzie (2011) provide size and flux estimates for some 23 SADs, the cumulative distribution curves of the *TRACE* data alone are very noisy, due to the sparseness of the sample. The *TRACE* measurements indicate that SADs smaller than SXT's resolution exist, so one can conclude that the frequency distribution below the range shown in Figure 1(a) is non-zero. However, combination of the SXT and *TRACE* measurements is made difficult by the vast differences in angular resolution and dynamic range (i.e., contrast),

which result in instrument-specific observational biases: as discussed in McKenzie & Savage (2009), the SAD areas measured from SXT may be systematically overestimated. In contrast, we find no reason to expect the flux density (i.e., magnetic field strength) to be limited by the observations. This is borne out by the observation that the 23 *TRACE* areas (ranging 1.9–12 Mm^2) and the 120 SXT areas (13–80 Mm^2) do not appreciably overlap, whereas the flux ranges overlap completely ($[3.9–45] \times 10^{17}$ Mx for *TRACE*, $[1.7–145] \times 10^{17}$ Mx for SXT). Thus, although the range of areas in the sample of 120 SADs is constrained by the SXT resolution, there appears to be no methodological limit on the SAD fluxes.

3. DISCUSSION

We propose that the distribution of sizes and fluxes reveals clues about the process which forms the SADs. Pursuant to the interpretation of SADs as reconnection products, the distribution of sizes and fluxes indicates the nature of some parameter(s) of localized (patchy and bursty) reconnection. As an extreme example, consider a scenario in which all the SADs were found to have identical sizes and fluxes. In such a case—which is not consistent with the present measurements—the implications for reconnection would be easy to define. In the present case interpretation is not as trivial, but is still possible. In the case of a log-normal distribution, for instance, it is not the sizes of SADs that are distributed normally, but the logarithm of the sizes. This can arise if, say, a reconnecting patch in the current sheet experiences growth at a rate that is proportional to the size of the patch:

$$\frac{dX}{dt} = kX. \tag{1}$$

Thus, the growth coefficient k is given by

$$\frac{d\ln(X)}{dt} = k, \tag{2}$$

and one can assume that the size is allowed to grow for some interval τ such that

$$X(\tau) = X_0 e^{k\tau}. \tag{3}$$

This argument follows exactly the discussion of Koch (1966) and requires each patch to grow from some initial "seed" size X_0. We find that $X(\tau)$ will be log-normally distributed if X_0 is log-normally distributed, or if k or τ is normally distributed. One possible configuration is to let the growth coefficient k be the same for all plasma voids, with the duration of the growth spurt being normally distributed. Such a scenario would a posteriori justify the combination of SAD measurements from 16 individual flares, since it presumes that all plasma voids grow at the same rate. (The opposite arrangement—normally distributed k and uniform τ—would also yield a log-normal $X(\tau)$; but it is more difficult to imagine all plasma voids having growth spurts of the same duration.)

In prior works (Savage & McKenzie 2011, and references therein) SADs have been interpreted as being created in a burst of reconnection at a localized patch in the current sheet beneath the coronal mass ejection and above the flare arcade. In that vein it is presumed that the size and flux of a SAD is determined by the reconnection rate during that localized burst (see also Linton & Longcope 2006). The scenario presented above then assigns k to some parameterization of the reconnection rate and leads to the supposition that k might be uniform for all reconnecting patches. While this appears to run counter to the concept that the reconnection rate is determined by the local microphysics, we note that the simulations of Shay et al. (2007) yielded nearly uniform reconnection rates for a nontrivial range of system sizes, aspect ratios, and ion/electron mass ratios. Additional numerical simulations of patchy reconnection may determine whether the prescription suggested above yields distributions of SAD sizes and fluxes similar to those found in the observations.

4. CONCLUSION

Pursuant to the idea that the characteristics of reconnection products should yield clues about the reconnection process, we have compared the measured sizes and estimated magnetic fluxes of SADs to four theoretical distribution functions. To avoid spurious variations in the distribution functions that may arise when data from multiple instruments are combined, we have examined only SADs measured with *Yohkoh*/SXT in 16 flares, at the expense of reduced spatial resolution and thereby reduced range in SAD sizes. We find that the cross-sectional areas of 120 SADs appear to follow a log-normal distribution, while the estimated magnetic fluxes are consistent with either a log-normal or an exponential distribution. The data are incompatible with a power-law distribution and thus do not appear to favor a fractal process for SAD creation.

The observed distribution of SAD sizes is likely affected by the processes of creation, fragmentation, and merging. Although fragmentation and merging may be possible for SADs, they have not been clearly observed in the coronal images to date. Future observations may provide evidence for fragmentation and/or merging, allowing empirical estimation of their relative importance.

In regards to creation of SADs, we offer a plausible scenario in which a log-normal distribution can be generated with minimal suppositions: First, the SADs form through patchy reconnection and grow at a rate described by Equation (1). Second, the growth coefficient k is approximately uniform for all SADs, while the duration of the growth is normally distributed. Although the conjecture of uniform k appears to imply a uniform reconnection rate for all resistive patches in supra-arcade current sheets, this scenario remains to be tested via numerical simulations of reconnection.

This work was partially supported by NASA under contract NNM07AB07C with the Harvard-Smithsonian Astrophysical Observatory. *Yohkoh* data are provided courtesy of the NASA-supported *Yohkoh* Legacy Archive at Montana State University. We gratefully acknowledge the helpful comments of an anonymous referee.

REFERENCES

Aschwanden, M. J., Dennis, B. R., & Benz, A. O. 1998, ApJ, 497, 972
Drake, J. F., Opher, M., Swisdak, M., & Chamoun, J. N. 2010, ApJ, 709, 963
Fermo, R. L., Drake, J. F., & Swisdak, M. 2010, Phys. Plasmas, 17, 010702
Innes, D. E., McKenzie, D. E., & Wang, T. 2003, Sol. Phys., 217, 247
Khan, J. I., Bain, H. M., & Fletcher, L. 2007, A&A, 475, 333
Koch, A. L. 1966, J. Theor. Biol., 12, 276
Linton, M. G., & Longcope, D. W. 2006, ApJ, 642, 1177
Longcope, D. W., McKenzie, D. E., Cirtain, J., & Scott, J. 2005, ApJ, 630, 596
McKenzie, D. E. 2000, Sol. Phys., 195, 381
McKenzie, D. E., & Hudson, H. S. 1999, ApJ, 519, L93
McKenzie, D. E., & Hudson, H. S. 2001, Earth Planets Space, 53, 577
McKenzie, D. E., & Savage, S. L. 2009, ApJ, 697, 1569
Nishizuka, N., Asai, A., Takasaki, H., Kurokawa, H., & Shibata, K. 2009, ApJ, 694, L74

Opher, M., Drake, J. F., Swisdak, M., Schoeffler, K. M., Richardson, J. D., Decker, R. B., & Toth, G. 2011, ApJ, in press
Press, W. H., Teukolsky, S. A., Vetterling, W. T., & Flannery, B. P. 1992, Numerical Recipes (Cambridge: Cambridge Univ. Press)
Savage, S. L., & McKenzie, D. E. 2011, ApJ, 730, 98
Savage, S. L., McKenzie, D. E., Reeves, K. K., Forbes, T. G., & Longcope, D. W. 2010, ApJ, 722, 329
Shay, M. A., Drake, J. F., & Swisdak, M. 2007, Phys. Rev. Lett., 99, 155002
Shibata, K., & Tanuma, S. 2001, Earth Planets Space, 53, 473